PROCEEDINGS OF SPIE

SPIEDigitalLibrary.org/conference-proceedings-of-spie

Improving visualization of cAMP gradients using algorithmic modelling

Howze, Patrick, Annamdevula, Naga, Phan, AnhVu, Pleshinger, D.J., Rich, Thomas, et al.

Patrick Howze IV, Naga Annamdevula, AnhVu Phan, D.J. Pleshinger, Thomas C. Rich, Silas J. Leavesley, "Improving visualization of cAMP gradients using algorithmic modelling," Proc. SPIE 11964, Imaging, Manipulation, and Analysis of Biomolecules, Cells, and Tissues XX, 119640M (3 March 2022); doi: 10.1117/12.2607772



Event: SPIE BiOS, 2022, San Francisco, California, United States

Improving Visualization of cAMP Gradients Using Algorithmic Modelling

Patrick Howze¹, Naga Annamdevula², AnhVu Phan⁴, D. J. Pleshinger^{2,3}, Thomas C. Rich², Silas J. Leavesley¹⁻³

¹Chemical and Biomolecular Engineering, University of South Alabama, AL 36688

²Pharmacology, University of South Alabama, AL 36688

³Center for Lung Biology, University of South Alabama, AL 36688

⁴Mechanical Engineering, University of South Alabama, AL 36688

ABSTRACT

A ubiquitous second messenger molecule, cAMP is responsible for orchestrating many different cellular functions through a variety of pathways. Förster resonance energy transfer (FRET) probes have been used to visualize cAMP spatial gradients in pulmonary microvascular endothelial cells (PMVECs). However, FRET probes have inherently low signal-to-noise ratios; multiple sources of noise can obscure accurate visualization of cAMP gradients using a hyperspectral imaging system. FRET probes have also been used to measure cAMP gradients in 3D; however, it can be difficult to differentiate between true FRET signals and noise. To further understand the effects of noise on experimental data, a model was developed to simulate cAMP gradients under experimental conditions. The model uses a theoretical cAMP heatmap generated using finite element analysis. This heatmap was converted to simulate the FRET probe signal that would be detected experimentally with a hyperspectral imaging system. The signal was mapped onto an image of unlabeled PMVECs. The result was a time lapse model of cAMP gradients obscured by autofluorescence, as visualized with FRET probes. Additionally, the model allowed the simulated expression level of FRET signal to be varied. This allowed accurate attribution of signal to FRET and autofluorescence. Comparing experimental data to the model results at different levels of FRET efficiency has allowed improved understanding of FRET signal specificity and how autofluorescence interferes with FRET signal detection. In conclusion, this model can more accurately determine cAMP gradients in PMVECs. This work was supported by NIH award P01HL066299, R01HL58506 and NSF award 1725937.

Keywords: Spectral, hyperspectral, FRET, gradients, cAMP, microscopy

1. INTRODUCTION

A diverse set of diseases, including COPD, CHF, asthma, and most recently COVID-19, directly and indirectly afflict the lungs. Lung disease is responsible for killing millions across the world each year. Hundreds of millions of people suffer from chronic respiratory diseases across the globe, and four million die prematurely from chronic respiratory disease every year¹. Respiratory disease is the leading cause of death in developing nations¹. 3'-5'-Cyclic adenosine monophosphate (cAMP) can play an integral role in these disease processes and further understanding the role of cAMP in a pathologic signaling setting is key to developing improved treatments and possible cures.

A ubiquitous second messenger molecule, cAMP is responsible for orchestrating many different cellular functions through a variety of pathways². A cyclic nucleotide, cAMP, regulates cellular functions such as gene transcription, cell growth and differentiation, and protein expression³. Recent experiments have demonstrated three dimensional cAMP gradients within cells and it is believed that the subcellular spatial distribution of cAMP may encode or dictate downstream physiology or pathophysiology. However, much remains unknown about the subcellular localization, kinetics, and frequency of cAMP signaling^{3,4}.

A standard class of sensors used to visualize localized cAMP concentrations are Förster resonance energy transfer (FRET) probes. These probes can target different intracellular locations but are limited by range and high background leading to a low signal-to-noise ratio³. Hyperspectral imaging has been used to overcome some of the limitations of FRET-based cAMP sensors^{5,6}. Hyperspectral imaging is an approach developed by NASA and initially for use in remote sensing. A hyperspectral imaging system acquires image data that is sampled over a wide range of wavelengths and measures contiguous spectral bands. This is useful because a hyperspectral imaging system acquires many more spectral bands than constituent species in a sample which allows for spectral discrimination between autofluorescence and background signals and the desired signal⁷. Though visibly measuring cAMP gradients has improved using hyperspectral imaging, this technique can still be degraded by electronic and biological noise. Previous experiments have demonstrated that spatial gradients in cAMP concentration can form as a result of specific agonist treatment in pulmonary

Imaging, Manipulation, and Analysis of Biomolecules, Cells, and Tissues XX, edited by Attila Tarnok, Jessica P. Houston Proc. of SPIE Vol. 11964, 119640M · © 2022 SPIE · 1605-7422 · doi: 10.1117/12.2607772

microvascular endothelial cells (PMVECs)⁴. PMVECs are specialized endothelial cells that line the microvasculature in the lung and play a key role in creating a semi-permeable barrier for alveolar gas exchange. PMVECs are responsible for optimal lung function. These results imply a connection between cAMP signaling specificity, spatial distribution of cAMP, and temporal changes in this distribution. Clearly, improved visualization of secondary messenger gradients is important to understanding the role of cAMP in regulating specific downstream processes. Despite the use of hyperspectral imaging techniques to isolate FRET signals, current visualization of cAMP gradients is complicated by competing sources of cellular and background autofluorescence and noise. Noise is generally defined as unwanted signal or meaningless information that can distort or even corrupt data. The presence of noise in imaging data obscures cAMP signals, making it difficult to determine exact cAMP gradient locations. Since FRET is a ratiometric measurement, and since measurement noise can affect both the donor and acceptor signals, this noise can have a compounding effect on FRET measurements.

Cellular autofluorescence is typically the largest competing signal when making FRET measurements⁴. A typical FRET probe consists of a molecular binding domain placed between a donor and acceptor fluorophore. In this case, when cAMP binds to the FRET probe a conformational change is triggered, causing the distance between donor and acceptor fluorophore to increase. The FRET efficiency, inversely proportional to the distance between donor and acceptor fluorophores, can then be measured using an appropriate imaging technique. But due to the low signal-to-noise ratio of FRET probes, their ability to accurately reflect cAMP distributions within cells is limited, which is further complicated by cellular autofluorescence. After cAMP binds to the probe, the distance between donor and acceptor increases, resulting in a decrease in acceptor emission and an increase in donor emission. Hyperspectral imaging has been employed to overcome some limitations of FRET imaging, such as competing autofluorescence and noise and the low signal-to-noise ratio of FRET probes.

In this research, to further understand the effects of noise on experimental data, a model was developed to simulate the presence of spatial distributions, or gradients, of cAMP concentration, and to assess the predicted experimental capability for accurately detecting cAMP spatial gradients. To achieve this, the model consisted of a theoretically generated cAMP spatial gradient that was implemented within the border of a 2-dimensional PMVEC, as defined by segmentation from experimental microscopy image data. The cAMP concentrations were converted to donor and acceptor emission intensities, as would be expected when using a hyperspectral imaging system to detect FRET probes experimentally. Donor and acceptor signals were mapped onto an image of unlabeled PMVECs which contained additional signals due to cellular autofluorescence and noise. The result was a time lapse model of cAMP gradients obscured by autofluorescence, as visualized with FRET imaging. Additionally, the model allowed the simulated expression level of the FRET reporter to be varied. This allowed estimation of the accuracy of FRET detection, as a function of competing autofluorescence, FRET efficiency, and FRET reporter expression. Results demonstrate that comparing experimental data to the model results at different levels of simulated expressiong of FRET reporter has allowed improved understanding of FRET signal specificity and how autofluorescence interferes with FRET signal detection.

2. METHODS

2.1 Cell Preparation

PMVECs were isolated from male Sprague Dawley rats by the University of South Alabama Center for Lung Biology cell culture core as described previously⁸. PMVECs were maintained in Dulbecco's Modified Eagle's Medium (DMEM; Life Technologies Inc., Carlsbad, CA) supplemented with 10% (vol/vol) fetal bovine serum (Gemini), 100 U/mL penicillin, and 100 ug/mL, pH 7.0. PMVECs were grown in 100 mm culture dishes in a humidified atmosphere of 5% CO2 and 95% air at 37°C. Confluent monolayers were passaged using 0.25% trypsin-EDTA (Invitrogen, Carlsbad, CA). PMVECs were transfected with a FRET sensor, pCDNA3 plasmid encoding H188 FRET-based cAMP probe, using 3.75 µl Lipofectamine 3000, 5 µl P3000 (Invitrogen), and 2.5 µg plasmid per well in serum-free media⁹. The H188 FRET sensor is comprised of a cAMP-binding domain obtained from exchange protein activated by cAMP (Epac) located between the donor fluorophore, Turquoise, and the acceptor fluorophore, Venus. Transfected cells were incubated at 37°C.

2.2 Spectral FRET Imaging

Spectral FRET imaging was performed similar to as previously described^{4,10}. Before imaging, coverslips were transferred to Attofluor holders (Thermo Fisher Scientific) and covered with 0.8 ml of extracellular buffer solution containing 145 mM NaCl, 4 mM KCl, 20 mM HEPES, 10 mM d-glucose, 1 mM MgCl2, and 1 mM CaCl2, at pH 7.3.

Using a Nikon A1R confocal microscope equipped with 60x water immersion objective (Plan Apo VC 60x DIC N2 WI NA-1.2; Nikon Instruments, Melville, New York) and 32 channel photomultiplier tube (PMT) spectral detector, spectral FRET images of PMVECs were obtained. Excitation wavelengths of 405 nm (8% laser intensity = 1.82 μ W at the sample stage) and 561 nm (10% intensity = 19.02 μ W at the sample stage) and emission wavelengths ranging from 414 to 724 nm in 10 nm increments were used for imaging. The 405 nm laser line was selected to excite the donor, Turquoise. Cells were selected for low, medium, and high FRET intensity levels. Baseline FRET (405 nm excitation) emission spectra were acquired for each image prior to addition of adenylyl cyclase activator forskolin (Calbiochem). Cells were exposed to 50 μ M forskolin for 10 min and the same fields of view were re-imaged using identical settings. Experiments were performed at room temperature (20-23°C).

2.3 Buildup of Model

To create the theoretical model, an autofluorescence image of a single non-transfected pulmonary microvascular endothelial cell (PMVEC) was selected. The selected image was converted to a binary mask image. A 2-dimnesional finite element analysis (FEA) approach was used to generate a theoretical cAMP heatmap with spatially-varying distributions of cAMP concentration (spatial cAMP gradients), as described previously 11. A custom MATLAB script was used to convert FEA-generated cAMP heatmaps to cAMP concentrations in image space. cAMP concentrations were then related to corresponding FRET efficiencies using the Hill equation and a Hill coefficient of 1. FRET efficiencies were then converted to relative signal levels of donor and acceptor fluorophores, assuming a constant expression level of the FRET reporter. The calculated donor and acceptor signals were then overlaid onto the original autofluorescence image. This process was repeated for each of the FEA analysis timepoints.

2.4 Comparing Model Results to Experimental Data

Model simulations were compared to experimental cAMP timelapse spectral image data to validate model results. Relative donor+acceptor intensity levels of 500, 700, and 1000 were evaluated. Experimental images were selected with approximately the same level of FRET reporter expression. The experimental and model images were compared based on summed autofluorescence and false-colored, linearly unmixed images⁴. Spatial variations in cAMP level were compared using line profiles while temporal variations were compared for selected regions of interest. At these same FRET efficiencies, a region of an experimental cell, model output without autofluorescence, and model output with autofluorescence were compared over time.

3. RESULTS AND DISCUSSION

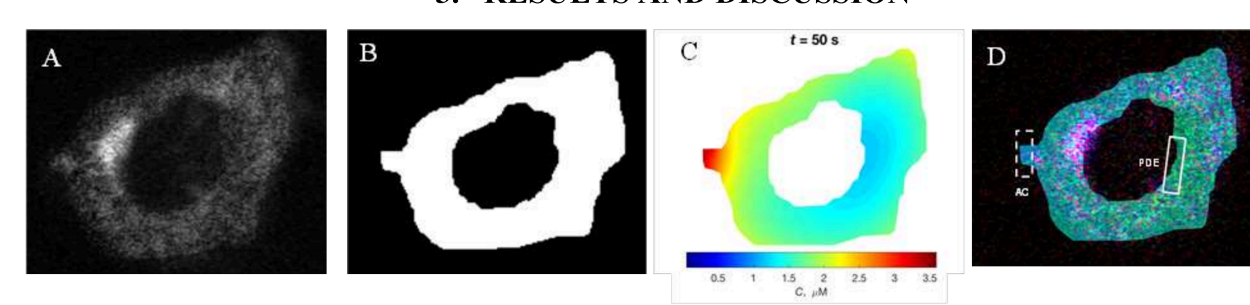


Figure 1. Build up and output of model. An autofluorescence image from an unlabeled PMVEC (A). A binary mask of this cell (B) was created. The binary mask was used as the basis to generate the theoretical finite element analysis simulation of cAMP signaling. A single time point (50 s) is displayed (C). An unmixed output from the model (D) is displayed. This output has been visualized as an overlay of the unmixed autofluorescence (red), unmixed donor (blue), and unmixed acceptor (green) fluorophores. Unmixed donor and acceptor signals were used to calculate relative cAMP concentration, which has been false colored for display.

The goal of this paper was to successfully build a model that simulate changes in cAMP concentration obscured by autofluorescence within a representative PMVEC. This model was then used to understand how contributions from autofluorescence and instrument noise affect measurement of FRET signal in single cell preparation and in turn how this affects the accuracy of visualizing cAMP gradients. To do this, a theoretical simulation of cAMP spatial spread within a single cell using finite element analysis based approach was utilized, as described previously¹¹. The simulation results were combined with experimentally measured image data of an unlabeled cell, containing signals from autofluorescence and instrument noise. To begin, a representative cell was selected that had a nonuniform distribution of autofluorescence

signal and instrument noise (F.1A). A binary mask of this cell was created that was then used as a basis for generating a finite element analysis model of cAMP distribution (F.1B). This allowed the FEA model to be generated within the same spatial context as the autofluorescent cell (F.1C). These were then overlayed (F.1D). In this segmented cell, the upper left region had a significant amount of autofluorescence, indicated by red, which likely obscured the FRET signal and made FRET measurements less accurate.

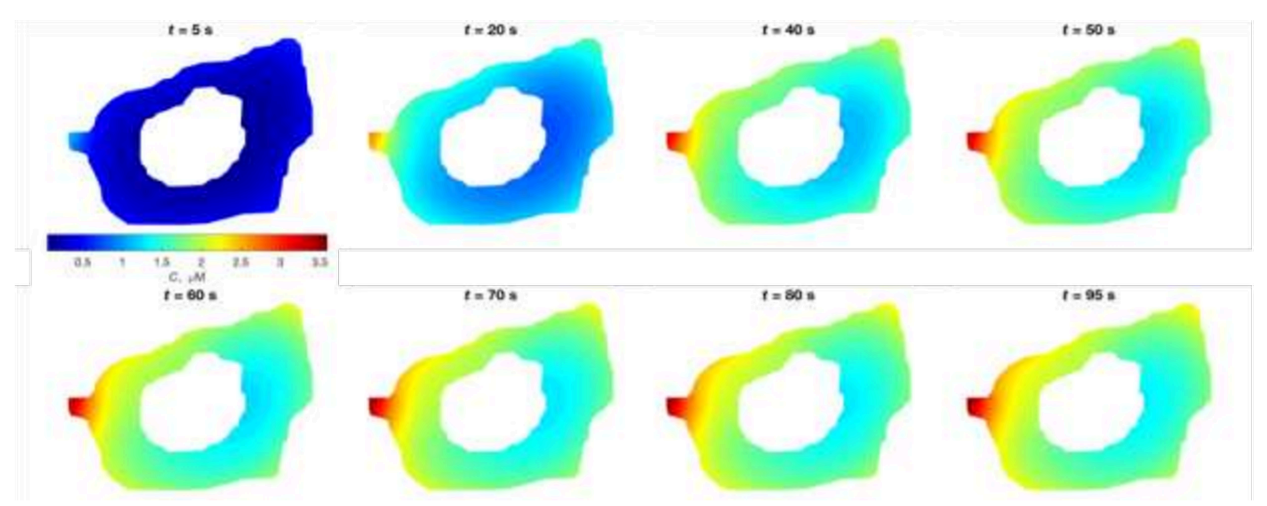


Figure 2. FEA generated cAMP heatmap over time in a PMVEC. Theoretical cAMP distributions were generated using finite element analysis and visualized using a JET colormap. A cAMP source (adenylyl cyclase) was simulated at the furthermost left point of the cell while cAMP sinks (phosphodiesterase) were simulated in the perinuclear region on the right side of the cell.

Figure 2 provides an expanded timeline for cAMP generation and degradation throughout the PMVEC as simulated using FEA. A cAMP source (adenylyl cyclase) was simulated at the left point of the cell while cAMP is degraded at the perinuclear region on the right side of the cell. As can be seen, the spatial variation in cAMP concentrations (spatial cAMP gradient) changes with each time point.

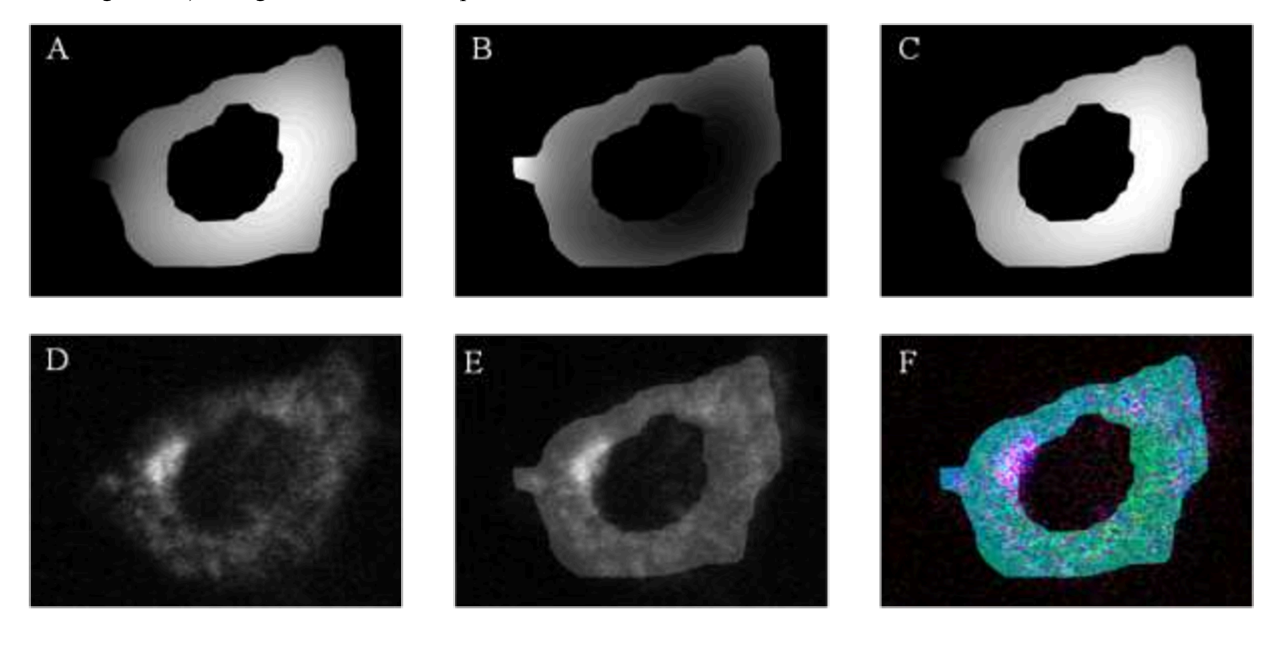


Figure 3. Model overlays. The FRET image (A) shows FRET efficiency mapped as a greyscale value. The turquoise (donor) (B) and venus (acceptor) were calculated from the FRET overlay by the code and used to generate the model. An unlabeled PMVEC was imaged as a source of experimentally relevant autofluorescence (D). The turquoise (B) and venus (C) overlays

were added to the unlabeled PMVEC (D). (F) shows a false colored image where the acceptor is represented by green, the donor is represented by blue, and autofluorescence is represented by red.

The simulation code processes each time point of the FEA generated cAMP heatmap and converts these images to grey scale images. The cAMP heatmap is then converted into a FRET efficiency image (F.4A). From this FRET image, the donor and acceptor overlays are extracted (F.4B, F.4C). These overlays are then added to the experimental image of the unlabeled PMVEC (F.4D) to give an output with donor and acceptor signal obscured by autofluorescent noise (F.4E). The final output is a series of images that simulate a changing level of cAMP, as described by FRET probes in a PMVEC. This model produces data like experimental data obtained in our lab.

4. CURRENT AND FUTURE WORK

FRET probes are powerful tools for studying intracellular signaling. Accurate measurement of intracellular FRET signal is complicated by autofluorescence. The results demonstrate that if the FRET signal is sufficiently high, accurate measurements can be made. cAMP measurements with weak FRET probe expression are likely unreliable. Current work involves comparing experimental data with the results produced from the model and assessing the accuracy of cAMP measurement given differing levels of autofluorescence. Future work will investigate noise contributions in addition to autofluorescence.

5. ACKNOWLEDGEMENTS

This work was supported by NIH award P01HL066299, R01HL58506, and NSF award 1725937. Drs. Leavesley and Rich disclose financial interest in a start-up company, SpectraCyte LLC, formed to commercialize spectral imaging technologies.

REFERENCES

- [1] Ferkol, T. & Schraufnagel, D. The Global Burden of Respiratory Disease. Annals ATS 11, 404–406 (2014).
- [2] Billington, C. K., Ojo, O. O., Penn, R. B. & Ito, S. cAMP Regulation of Airway Smooth Muscle Function. Pulm Pharmacol Ther 26, 112–120 (2013).
- [3] Rich, T. C., Webb, K. J. & Leavesley, S. J. Can we decipher the information content contained within cyclic nucleotide signals? J Gen Physiol 143, 17–27 (2014).
- [4] Annamdevula, N. S. et al. Spectral imaging of FRET-based sensors reveals sustained cAMP gradients in three spatial dimensions: 4D spectral imaging of FRET-based sensors. Cytometry 93, 1029–1038 (2018).
- [5] Levy, S. et al. SpRET: Highly Sensitive and Reliable Spectral Measurement of Absolute FRET Efficiency. Microscopy and Microanalysis 17, 176–190 (2011).
- [6] Leavesley, S. J., Britain, A. L., Cichon, L. K., Nikolaev, V. O. & Rich, T. C. Assessing FRET using spectral techniques. Cytometry Part A 83, 898–912 (2013).
- [7] Leavesley, S. J. et al. HyperSpectral imaging microscopy for identification and quantitative analysis of fluorescently-labeled cells in highly autofluorescent tissue. J Biophotonics 5, 67–84 (2012).
- [8] Stevens, T., Creighton, J. & Thompson, W. J. Control of cAMP in lung endothelial cell phenotypes. Implications for control of barrier function. American Journal of Physiology-Lung Cellular and Molecular Physiology 277, L119–L126 (1999).
- [9] Klarenbeek, J., Goedhart, J., van Batenburg, A., Groenewald, D. & Jalink, K. Fourth-Generation Epac-Based FRET Sensors for cAMP Feature Exceptional Brightness, Photostability and Dynamic Range: Characterization of Dedicated Sensors for FLIM, for Ratiometry and with High Affinity. PLoS One 10, e0122513 (2015).
- [10] Annamdevula, N. S. *et al.* Measurement of 3-Dimensional cAMP Distributions in Living Cells using 4-Dimensional (x, y, z, and λ) Hyperspectral FRET Imaging and Analysis. *JoVE (Journal of Visualized Experiments)* e61720 (2020) doi:10.3791/61720.
- [11] Stone, N., Shettlesworth, S., Rich, T. C., Leavesley, S. J. & Phan, A.-V. A two-dimensional finite element model of cyclic adenosine monophosphate (cAMP) intracellular signaling. SN Appl. Sci. 1, 1713 (2019).